RSC Advances

PAPER

View Article Online
View Journal | View Issue

Cite this: *RSC Adv.*, 2016, **6**, 24203

Utilization of solar energy for continuous bioethanol production for energy applications†

Betina Tabah,[a] Indra Neel Pulidindi,[a] Venkateswara Rao Chitturi,[c] Leela Mohana Reddy Arava[c] and Aharon Gedanken*[ab]

Received 6th January 2016
Accepted 26th February 2016

DOI: 10.1039/c6ra00389c

www.rsc.org/advances

The focus of the present research is to develop energy-efficient, sustainable, and continuous-flow bioethanol production based on solar energy. Solid-state fermentation of glucose was performed in a specially designed solar-energy-driven continuous flow reactor. Aqueous glucose solutions of 10 and 20 wt% were fed into the reactor bed containing baker's yeast (*Saccharomyces cerevisiae*), resulting in 4.7 and 8.7 wt% ethanol yields, respectively. The bioethanol produced was separated from the yeast bed soon after its formation by an evaporation–condensation process. High ethanol yields (91.2 and 85.5% of the theoretical yield, respectively) indicate the atom-efficiency of the process. No loss in the activity of yeast was observed even after two months of continuous operation of the reactor. The current study demonstrates an energy-efficient methodology for bioethanol production utilizing solar energy. The bioethanol obtained (8.7 wt%, *ca.* 2 M) was further tested in alkaline-acid direct ethanol fuel cells operated at 303 K, resulting in a power density value of 330 mW cm^{-2} at a modest open circuit voltage value of 1.65 V (65.5% voltage efficiency).

Introduction

Bioethanol production is important not only because it could be blended with gasoline but also it could be a feedstock for the production of C_2 hydrocarbons. In near future, biofuels, especially bioethanol and biobutanol, could form the vital feedstock for long-chain hydrocarbons and also for a variety of biochemicals that are currently solely being produced from oil.[1,2] The potential global production of bioethanol from crop wastes and crop residues is estimated at 491 GL per year, which could replace 32% of total gasoline consumption.[3] Bioethanol, because of its high gravimetric energy density (30 MJ kg^{-1}), high octane value, and high combustion efficiency (the anti-knock index for gasoline: 87, for ethanol: 99), is one of the most promising alternatives to conventional transportation fuels.[4,5] In addition, the use of ethanol produced from biomass as a transport fuel can reduce CO_2 buildup.[6] Bioethanol can be blended with petrol or used as neat alcohol in dedicated engines and it is an excellent fuel for advanced future flexible-fuel hybrid vehicles.[7] In comparison to gasoline, ethanol contains only a trace of sulfur; therefore, ethanol blended with gasoline helps to decrease the overall emission of SO_x.[8] Global annual bioethanol production reached nearly 115 billion liters in 2015.[9] Hence, breakthroughs in bioethanol production technologies are beneficial for the socio-economic well-being of humankind.

Bioethanol production, using various substrates by free or immobilized cells of bacteria (*Clostridium* sp.) or yeasts (*Saccharomyces* sp., *Zymomonas* sp.), has been intensively studied over the past two decades. Fermentation using immobilized cells prevent substrate inhibition. In immobilized systems, the use of higher concentrations of carbohydrates is feasible and the recovery of the biocatalysts is simple; therefore, the biocatalysts can be reused for many fermentation cycles.[10] *Saccharomyces cerevisiae* is a facultative anaerobe able to live on various fermentable and non-fermentable carbon sources. When it is grown on fermentable substrates, such as glucose, the metabolic energy originates from glycolysis.[11] Additionally, *S. cerevisiae* is the most effective ethanol-producing microorganism for hexose sugars including glucose, mannose, and galactose. *S. cerevisiae* is a yeast with high ethanol productivity, high tolerance to ethanol and to the inhibitory compounds present in the hydrolysate of lignocellulosic biomass.[12]

[a]*Department of Chemistry, Bar-Ilan University, Ramat-Gan 52900, Israel. E-mail: gedanken@mail.biu.ac.il; Fax: +972-3-7384053; Tel: +972-3-5318315*

[b]*Department of Materials Science and Engineering, National Cheng Kung University, Tainan 70101, Taiwan*

[c]*Department of Mechanical Engineering, Wayne State University, Detroit, MI 48202, USA*

† Electronic supplementary information (ESI) available: Design of the solar reactor (Fig. S1), theoretical yield of ethanol from glucose fermentation (eqn (S1)), ^{13}C NMR spectrum of authentic glucose (Fig. S2), ^{1}H NMR spectra of authentic glycerol and acetic acid (Fig. S3), ^{13}C NMR spectra of authentic glycerol and acetic acid (Fig. S4), comparison of ethanol concentrations deduced from GC and ^{1}H NMR analyses from 10 and 20 wt% glucose fermentation (Tables S1 and S2), powder XRD patterns recorded for bimetallic Pd catalysts (Fig. S5), and AA-DEFC performances reported in the literature (Table S3). See DOI: 10.1039/c6ra00389c

A common problem in bioethanol production is the separation of microorganisms from the broth. Solid-state fermentation is the fermentation involving solids in absence (or near absence) of free water. However, substrates must have enough moisture to support growth and the metabolism of microorganisms. Solid-state fermentation, with its low energy requirements, produces less wastewater and is environment-friendly. In addition, in solid-state fermentation, microbial cultures are closer to their natural habitats and it is easy to separate them from the broth.[13]

Solar energy is a sustainable energy source and exploiting it for biofuels production has economic and environmental advantages. Thus, the use of alternate green, sustainable, and renewable resources such as biomass and solar energy could be a solution to meet the growing energy demands. To the best of our knowledge, we are the first to utilize solar energy for bioethanol production.[14] The objective of the present study is to develop a continuous flow solid-state glucose fermentation process driven by solar energy for production of bioethanol in a specially-designed reactor. The special design of the reactor facilitated *in situ* separation of ethanol from the yeast bed by evaporation–condensation process. Moreover, the bioethanol produced was demonstrated as a potential fuel for operating direct ethanol fuel cells.

Experimental

The solar reactor

The solar reactor was designed and fabricated to perform solid-state glucose fermentation (flow system) and to continuously separate the aqueous ethanol solution from the yeast bed by an *in situ* evaporation–condensation mechanism (Fig. 1). Two aspects, namely, the geometry and the dimensions were crucial in the operation of the reactor for effective production as well as separation of ethanol. The reactor was fabricated using aluminum blocks so that it was lightweight and non-corrosive. A nearly right-angle triangular geometry (with 275 mm base and 127 mm height) was selected. The height of the reactor was kept much lower than the base to facilitate the condensation of ethanol vapor (from the first chamber) onto the top glass surface. Such geometry facilitated free flow of the condensate from the top surface of the reactor to the second chamber, where ethanol was collected (see ESI, Fig. S1† for a detailed design and depiction of the components of the solar reactor). Tabah *et al.* previously reported the principle of operation of the reactor.[14]

Solid-state glucose fermentation

Glucose (D-glucose, product no. G8270, Sigma-Aldrich, Israel) solution reservoir (2 L, 10 or 20 wt%), was connected to the solar fermentation reactor (Fig. 1a). The first chamber of the reactor had 75 g of *Saccharomyces cerevisiae* (instant baker's yeast purchased from the local supermarket) covered with activated carbon cloth (Kynol®, 90 g m^{-2}, 0.43 mm thickness, >1800 m^2 g^{-1} specific surface area) (Fig. 1b) into which the glucose solution was continuously fed (2.8 mL h^{-1} flow rate). The yeast was not supplemented with any other additional nutrients and the pH of the glucose solutions was 7. Fermentation took place in this chamber and the ethanol produced was evaporated to the top flat glass surface of the reactor, which allowed the solar radiation into the bed. The ethanol droplets that condensed on the glass plate were collected in the second chamber of the reactor, which had an outlet for ethanol collection (see ESI, Fig. S1† for the design of the solar reactor).

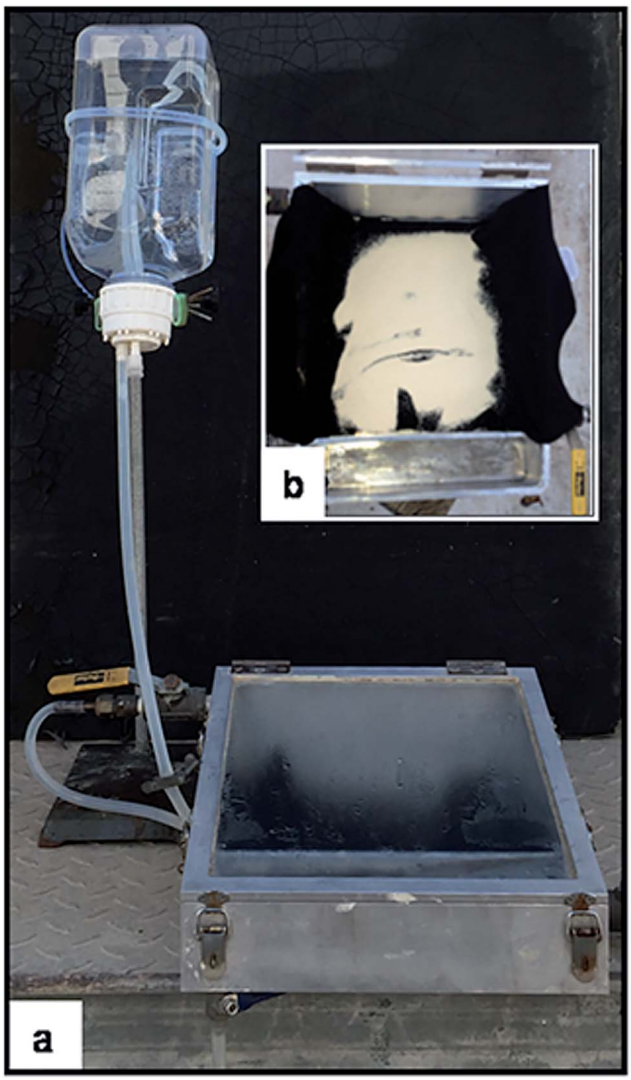

Fig. 1 Solar reactor (whole system) (a), open reactor with instant baker's yeast on activated carbon cloth (b).

^{1}H and ^{13}C NMR analyses

Aliquots were collected from the reactor (ethanol outlet) at regular time intervals and analyzed by ^{1}H and ^{13}C NMR spectroscopy. D_2O was used as a solvent and spectra were recorded on Bruker Avance DPX 300 at room temperature. HCOONa (97%, product no. 107603, Sigma Aldrich, Israel) was used as an internal standard in ^{1}H NMR spectroscopy for quantification of ethanol.[14,15]

Gas chromatography (GC) analysis

The quantification of ethanol present in the product was also performed by gas chromatography (Gas chromatograph Varian

3900). The GC was equipped with a Varian Chrompack capillary column (25 m × 0.63 mm × 10 μm) and a flame ionization detector (FID). The detector temperature was fixed at 200 °C and helium was used as a carrier gas. The initial oven temperature was 80 °C for 0.5 min, reaching 160 °C with a heating rate of 20 °C min^{-1} and remaining at this temperature for 10 min. The column oven end time was 14.5 min. The injection temperature was 140 °C (with a split ratio of 50 and column flow 2.0 mL min^{-1}). 10 μL of sample was injected into the chromatograph during each analysis. The chromatograms were recorded and the peak responses were measured. Product identification was done by comparing the retention time of the analyte with that of the authentic sample. The ethanol yield was calculated from the calibration plot deduced from standard ethanol (AR, Cat. no. 05250502, BioLab, Israel).

Preparation of 30 wt% Pd_1Ni_1/C and 50 wt% Pd_1Au_1/C electrocatalysts

Bimetallic palladium electrocatalysts were prepared by $NaBH_4$ reduction method. Metal salts, specifically K_2PdCl_4, $HAuCl_4 \cdot 3H_2O$, and anhydrous $NiCl_2$ were used as precursors. In a typical synthesis, desired amounts of metal salts were dissolved in ethylene glycol and added to the vulcan XC-72 carbon dispersed in ethylene glycol. The resulting suspension was then stirred for 1 h. Thereafter, $NaBH_4$ dissolved in ethylene glycol was added slowly under continuous stirring at room temperature. After 3 h, the suspension was filtered, washed thoroughly with ethanol and dried under vacuum. Finally, the materials were heat-treated at 773 K under H_2/N_2 (9 : 1) for 1 h. The prepared materials were characterized using X-ray diffraction (XRD-Rigaku Miniflex II), scanning electron microscopy (SEM-JEOL JSM-7500F), and transmission electron microscopy (TEM-JEOL JEM 2010) techniques.

Membrane electrode assembly (MEA) fabrication

The as-synthesized 30 wt% Pd_1Ni_1/C and 50 wt% Pd_1Au_1/C catalysts were used to fabricate three-dimensional (3D) structured anode and cathode, respectively. Briefly, a homogeneous mixture consisted of Pd_1M_1/C (M = Ni and Au), isopropanol, and 5 wt% Nafion was spray-coated on the 3D macroporous Ni foam layer-wise and dried. The active material loading on the anode and cathode was maintained to be 1.0 and 3.5 mg cm^{-2}, respectively. MEA was fabricated by sandwiching cation exchange membrane (pre-treated Nafion 211, 25 μm thickness) between anode and cathode. Pre-treatment of Nafion 211 was conducted by immersing it in 10 wt% NaOH solution and heating at 353 K for 1 h followed by washing with de-ionized water several times.

Alkaline-acid direct ethanol fuel cell (AA-DEFC) measurements

During the operation of fuel cell, alkalized bioethanol (2 M bioethanol + 5 M NaOH) and acidified hydrogen peroxide (4 M H_2O_2 + 1 M H_2SO_4) were fed at anode and cathode, respectively. Flow rate of both bioethanol and hydrogen peroxide was maintained to be 2 mL min^{-1} using peristaltic pump and performance of the fuel cell was measured at two different temperatures, 303 and 333 K. The MEA was conditioned at a constant current density until the open circuit voltage (OCV) became steady and then current–voltage (*I–V*) polarization curves were recorded by applying potential from OCV to 0.2 V.

Results and discussion

Continuous flow bioethanol production in a solar energy-driven reactor

The maximum theoretical yield of ethanol expected from the fermentation of 10 wt% glucose solution is 5.1 wt% and of 20 wt% glucose solution is 10.2 wt% (see ESI, eqn (S1)†). However, due to different metabolic pathways operative in the yeast, in addition to ethanol, secondary metabolites such as glycerol and acetic acid are also formed reducing the process efficiency. The concentration of aqueous ethanol collected at regular time intervals using 10 and 20 wt% glucose feed are plotted in Fig. 2. The average ethanol yield from 10 wt% glucose feed was 4.7 ± 0.2 wt% (1 M, 91.2% of the theoretical yield) and from 20 wt% glucose feed was 8.7 ± 0.9 wt% (1.9 M, 85.5% of the theoretical yield). The high yields of ethanol could be due to the provision in the reactor for the *in situ* separation of ethanol from the fermentation broth which facilitates the forward reaction of ethanol formation in accordance with Le Chatelier's principle. Since all the experiments were performed during winter (mid December to mid February), the average temperature was 20 °C during the day and 13 °C during the night. Although the fermentation was continuous, majority of the evaporation process occurred during the day and was negligible during the night.

After reaching maximum ethanol yield possible with 10 wt% glucose feed, the reactor was then fed with 20 wt% aqueous glucose solution with the same yeast bed for another month. No loss in the activity of yeast was observed even after two months of continuous operation of the solar-energy driven fermentation reactor with different glucose feed solutions. Unlike the

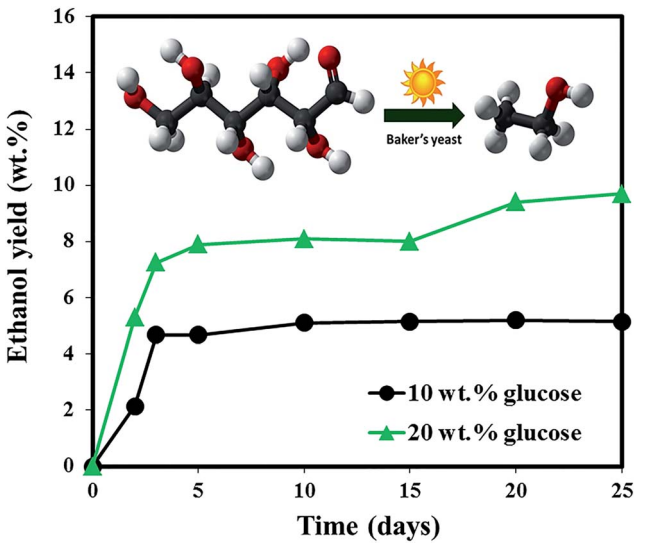

Fig. 2 Time on stream studies of ethanol yield (wt%) with 10 and 20 wt% glucose feed solutions (T_{ave}: 20 °C/13 °C).

cultured yeasts grown in the laboratory, the yeast strain used in the current experiments is the commercial instant baker's yeast. Moreover, the yeast was taken in large excess which could be the reason for the sustained activity for two months utilizing a sole carbon source, glucose. It should be noted that the yeast bed was always in solid state, thus there was no effluent and it was very convenient to change the feed solutions between the experiments.

Increasing the concentration of glucose feed also increased the ethanol yield (from 4.7 wt% to 8.7 wt%) indicating the efficiency of the fermentation process, resulting in bioethanol yields close to the theoretical values (91.2 and 85.5% of the theoretical yield, respectively). Representative ^{1}H NMR spectra of the ethanol produced from 10 and 20 wt% aqueous glucose solutions (collected on 25th day) are shown in Fig. 3. A peak centered at 1.19 ppm (3H, t) and a peak centered at 3.66 ppm (2H, q) are typical of the presence of ethanol. The singlet peak at 8.40 ppm is attributed to HCOONa, an internal standard used to quantify ethanol amount, and the peak at 4.80 ppm corresponds to the solvent.

In addition to ^{1}H NMR, the product was also analyzed by ^{13}C NMR spectroscopy. Typical ^{13}C NMR spectra of the product obtained from 10 and 20 wt% aqueous glucose feed solutions (collected on 10th day) are depicted in Fig. 4a and b with comparison to authentic ethanol (Fig. 4c). The characteristic peaks of $-CH_3$ group at 17 ppm and $-OCH_2$ group at 58 ppm indicate that ethanol is the only fermentation product. No trace of glucose (61 (C6), 70 (C4), 72, 73 (C2), 75 (C3), 76 (C5), 92 ($C1_\alpha$), and 96 ($C1_\beta$) ppm) was observed in the product (see ESI, Fig. S2† for ^{13}C NMR spectrum of authentic glucose). The absence of glucose or yeast in the product signifies the role of solar radiation in separating the aqueous ethanol formed in the fermentation chamber by means of evaporation and condensation processes. Absence of typical peaks of secondary metabolites, glycerol and acetic acid, in both ^{1}H NMR (Fig. 3a and b) and ^{13}C NMR (Fig. 4a and b) spectra of the fermentation product again indicates the product purity and its possible direct use for energy related applications such as fuel cells operation (see ESI, Fig. S3 and S4† for ^{1}H and ^{13}C NMR spectra of authentic glycerol and acetic acid).

Moreover, the fermentation products were further analyzed using GC. The chromatograms of the aliquots of products from 10 and 20 wt% glucose feeds collected on 25th day of the fermentation are shown in Fig. 5a and b. For comparison, the chromatogram of authentic ethanol is also shown in Fig. 5c. The appearance of the peak at 6.9 min retention time in both analytes confirms the presence of ethanol. The ethanol yields from 10 and 20 wt% glucose feed on 25th day were calculated (from the calibration plot) as 4.8 wt% (1 M) and 8.5 wt% (1.9 M), respectively. The concentration of the analytes determined from GC analyses agreed well with ^{1}H NMR analyses confirming the authenticity of the methodology used for ethanol estimation (see ESI, Tables S1 and S2† for comparison).

Novel methods have been explored for bioethanol production by various research groups for making the processes commercially feasible.[16] Pulidindi *et al.* reported 2.3 times increase in the fermentation rate of glucose (20 wt%) using sonication (compared to a stirred reaction).[17] Tabah *et al.* studied the effect of stirring speed on the kinetics of glucose (20 wt%) fermentation and reported two times enhancement of fermentation rate using an ultraturrax compared to the incubation at 30 °C. The acceleration of fermentation was also observed using other carbohydrates such as sucrose and molasses.[15] Choi *et al.* reported a maximum of 31.6% ethanol yield from starch using fermentative bacteria in their study about fermentative bioenergy production using ultrasonication on microalgae biomass *Scenedesmus obliquus*.[18] Nakashima *et al.* developed a direct bioethanol production from cellulose by arming yeast using ionic liquid pretreatment, producing approximately 90% ethanol yield.[19] Saifuddin and Hussain studied microwave assisted bioethanol production from starch and improved the yield of ethanol by 45.5% when compared to the non-microwave process.[20] Despite being novel, all the abovementioned methods are based on highly-controlled reactions and state-of-the-art instruments requiring electrical energy input.

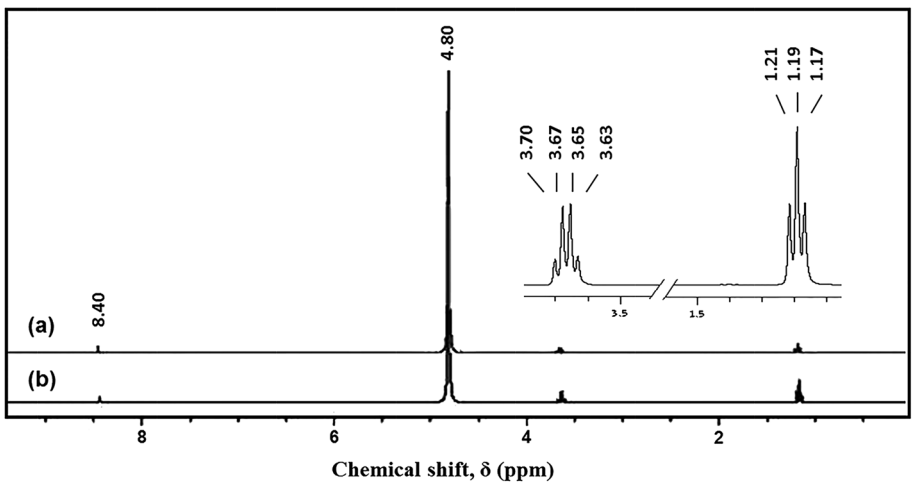

Fig. 3 ^{1}H NMR spectra of ethanol produced from (a) 10 wt% glucose (collected on 25th day, 1.1 M) and (b) 20 wt% glucose (collected on 25th day, 2.1 M) feed solutions (inset shows the ethanol peaks, a 3H (t) centered at 1.19 ppm and a 2H (q) centered at 3.66 ppm).

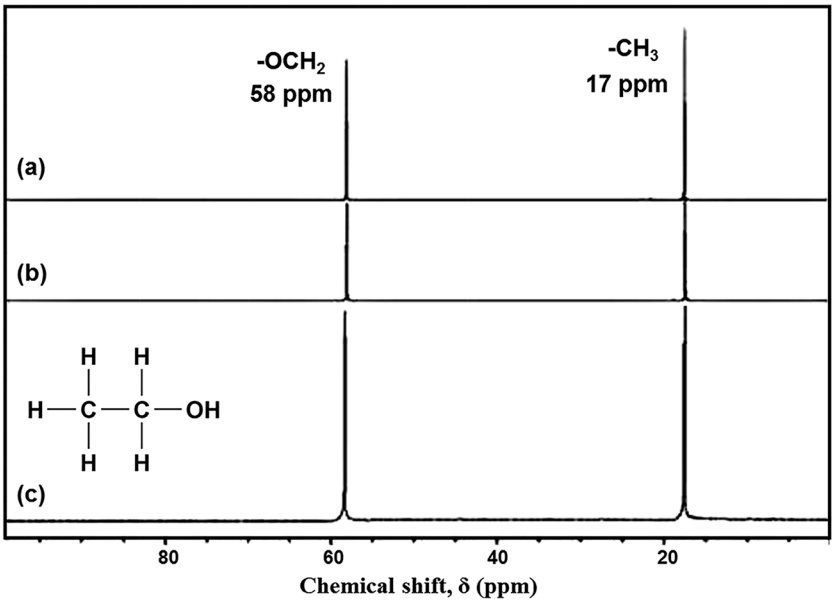

Fig. 4 ^{13}C NMR spectra of (a) ethanol from 10 wt% glucose solution (collected on 10th day, 1.1 M), (b) ethanol from 20 wt% glucose solution (collected on 10th day, 1.8 M), and (c) authentic ethanol.

In our previous study, we reported 84% of theoretical yield for conversion of starch (5 wt%) to ethanol in a single step batch fermentation process by using the solar reactor at 30–35 °C.[14] In the current study, not only solar energy was used to obtain close to theoretical ethanol yields (91.2 and 85.5%) from the glucose feeds (10 and 20 wt%) but also the bioethanol production was a continuous flow solid-state process. Even though solar energy is unstable in terms of limited day hours and seasons, the present study demonstrates the operability and the sustainability of the process even in winter season with lower temperatures (20 °C). Moreover, no electricity was consumed for the operation of the fermentation reactor making the whole process green, sustainable, and most importantly cost effective. Thus, this process is economically feasible, having no energy requirement other than solar energy – which is free – for bioethanol production.

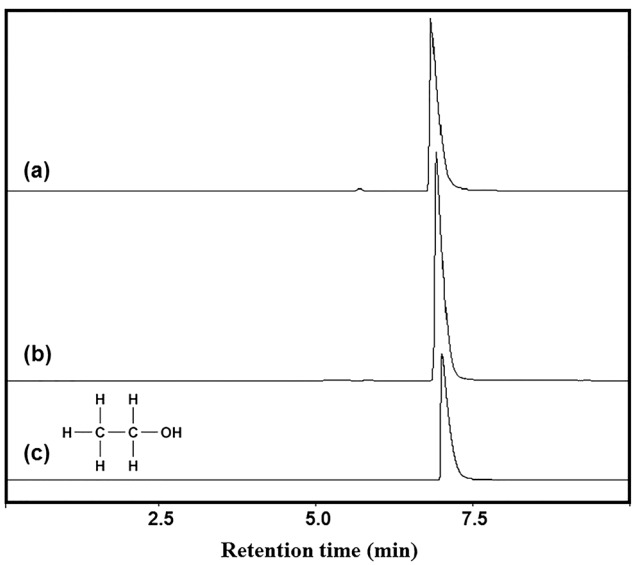

Fig. 5 Gas chromatograms of (a) ethanol from 10 wt% glucose solution (collected on 25th day, 1 M), (b) ethanol from 20 wt% glucose solution (collected on 25th day, 1.9 M), and (c) authentic ethanol.

One of the main issues associated with bioethanol production is its purification from fermentation broth.[21] Various approaches for extraction and distillation of ethanol are being studied.[21,22] It is important to note that, although further distillation is needed to attain anhydrous ethanol, the unique advantage of the use of solar energy in the current methodology is that no additional extraction process is required to separate the aqueous ethanol from the fermentation broth. The formed ethanol in the yeast bed is simultaneously evaporated and condensed to the glass panel of the reactor from which it flows down into a separate chamber with an outlet for ethanol collection. The lower pressure in the reactor, relative to the atmospheric pressure, facilitates the evaporation of ethanol at a temperature much lower than the boiling point of ethanol (78.5 °C). Lowering of boiling point of ethanol as a function of its vapor pressure and the principle of operation of the reactor were described by Tabah *et al.*[14] A maximum of 8.72 wt% (~2 M) ethanol was produced in the current process through fermentation of 20 wt% glucose solution and the potential of the bioethanol generated was tested for fuel cell applications.

Alkaline-acid direct ethanol fuel cell (AA-DEFC) performance at 303 and 333 K

AA-DEFCs have drawn much attention due to the high power density, faster kinetics of ethanol oxidation in alkaline media, low activation loss and faster kinetics of hydrogen peroxide reduction in acidic media due to two-electron transfer, use of non-Pt electrocatalysts, low fuel cross-over and high theoretical

cell voltage (2.52 V) than other types of fuel cells.[23–25] These fuel cells are characterized by oxidation of ethanol at anode ($CH_3CH_2OH + 12OH^- \rightarrow 2CO_2 + 9H_2O + 12e^-$; $E^o = -0.74$ V) and reduction of hydrogen peroxide at cathode ($6H_2O_2 + 12H^+ + 12e^- \rightarrow 12H_2O$; $E^o = +1.78$ V). Different electrocatalysts were explored to improve the kinetics of redox reactions and thereby the power density.[24,26,27] Recently, Zhao's research group demonstrated a high power density of 360 mW cm^{-2} at 333 K using PdNi/C at anode with a loading of 1.0 mg cm^{-2} and Pt/C at cathode with a loading of 3.9 mg cm^{-2}.[24] In the present work, PdNi/C was used for the oxidation of bioethanol at anode and PdAu/C for the reduction of hydrogen peroxide at cathode. The reason for using PdAu/C rather than Pt/C is to avoid the decomposition of hydrogen peroxide into oxygen and water.[28,29] Moreover, it is less expensive than Pt.[30]

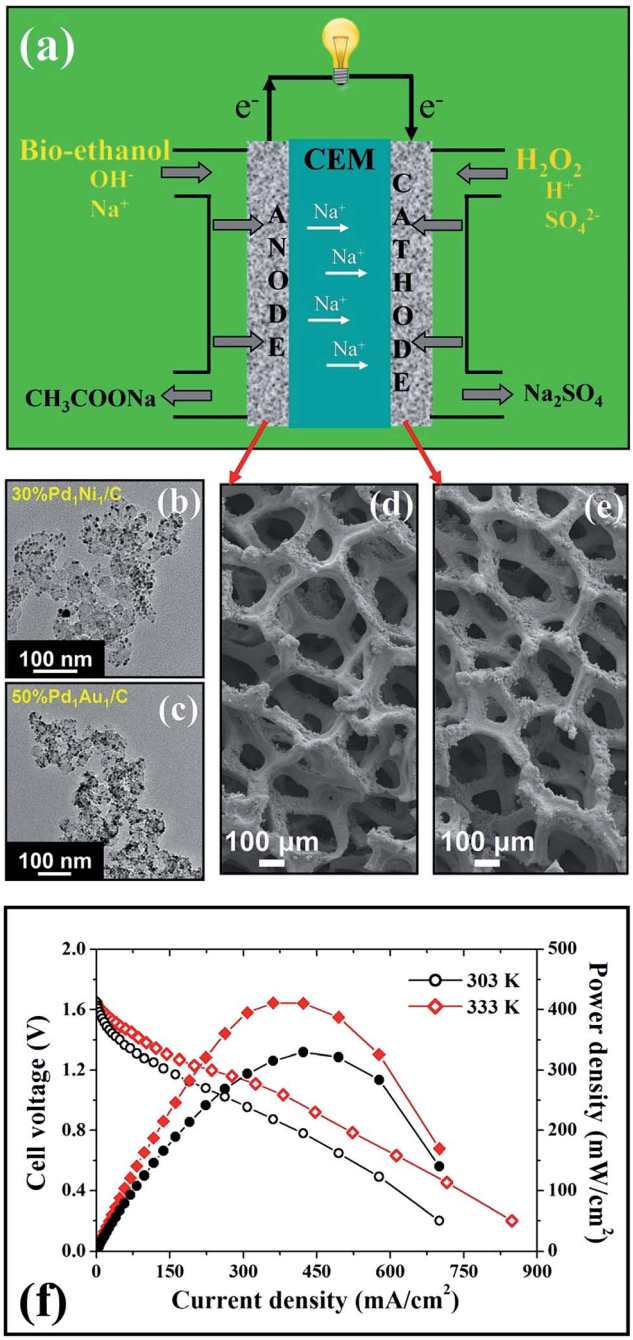

Fig. 6 Schematic representation of AA-DEFCs operated with as-produced bioethanol as fuel (a), TEM images of bimetallic Pd electrocatalysts (b and c), SEM images of 3D-structured anode and cathode (d and e), and current–voltage (*I–V*) polarization and power density curves recorded at 303 and 333 K (f).

Schematic representation of AA-DEFCs is depicted in Fig. 6a. The system is composed of alkalized bioethanol and acidified hydrogen peroxide compartments separated by a cation conducting membrane. In both anode and cathode compartments, 3D-structured electrodes were used to facilitate the diffusion of reactant species and also improve the electrochemical active surface area for redox reactions. XRD analysis confirmed phase purity of the materials (see ESI, Fig. S5†). Particle size was observed to be *ca.* 5–6 nm for 30 wt% Pd_1Ni_1/C and 50 wt% Pd_1Au_1/C catalysts based on TEM images (Fig. 6b and c) and the 3D-structured configuration of the electrodes was seen from SEM images (Fig. 6d and e).

I–V polarization and power density curves of AA-DEFCs operated at 303 and 333 K are shown in Fig. 6f. The open circuit voltage (OCV) was observed to be around 1.65 V (*i.e.* 65.5% voltage efficiency) at both operating temperatures. A maximum power density of 330 mW cm^{-2} was observed at 303 K. The OCV and power density observed in AA-DEFCs configuration is higher than the values reported in the literature for acid DEFCs and alkaline DEFCs.[14,30–32] The improved performance can be attributed to the avoidance of the mixed-potential phenomena. When the operating temperature increased from 303 to 333 K, the power density increased from 330 to 410 mW cm^{-2}. The enhanced performance is attributed to the faster electrochemical kinetics of the redox (ethanol oxidation and H_2O_2 reduction) reactions at the electrode compartments, improved membrane conductivity, increased reactant delivery and product removal rates. The performance values observed in the present study are higher than the values reported in literature (see ESI, Table S3† for comparison). This is possibly due to the high catalytic activity of bimetallic Pd electrocatalysts and 3D-structured electrode configuration.

The superior features of the current approach for bioethanol production and its application are (i) the bioethanol production process being a continuous flow which could be easily adopted for industrial applications for large scale production, (ii) obtaining high concentrations of bioethanol (~2 M) by feeding 20 wt% glucose solution into the reactor, (iii) using solar energy for fermentation and for separation of the formed ethanol, (iv) achieving high ethanol yields without electricity consumption, (v) using the same microorganism (without any additional nutrients) for a long time (two months) without loss in the activity, (vi) no production of any polluting effluent due to the solid-state fermentation, (vii) demonstrating the potential of the produced bioethanol as fuel for operating AA-DEFCs, and (viii) achieving current and power density values as high as 700 mA cm^{-2} and 330 mW cm^{-2} at a modest OCV of 1.65 V.

Conclusions

Biofuels may replace current transportation fuels and the major commercial biofuel is bioethanol. A solar-energy driven solid-state continuous flow bioethanol production process was described in the current study. Solar energy was not only used to drive the glucose fermentation reaction but also to separate the bioethanol *in situ* from the broth. Separation of ethanol from the yeast bed was possible soon after its formation by an evaporation–condensation process. No traces of the reactant (glucose) or secondary metabolites (glycerol or acetic acid) were observed in the product. The average ethanol yield was 91.2 and 85.5% of the theoretical yield for 10 and 20 wt% of glucose solutions, respectively. Thus, even at low operation temperatures (~20 °C), solar-energy based solid-state fermentation is a promising method for bioethanol production. In addition to the production of 2 M bioethanol from 20 wt% glucose feed, the application of this bioethanol was demonstrated for the operation of the DEFCs. The OCV was observed to be 1.65 V which corresponds to 65.5% voltage efficiency. The current and power density values derived from the fuel cell operated at room temperature were 700 mA cm^{-2} and 330 mW cm^{-2}, respectively. Thus, a new avenue was explored for decentralized power supply based on solar energy. Preliminary studies also revealed successful results with higher amounts of glucose feed (14 wt% ethanol from 30 wt% glucose solution and 18 wt% ethanol from 40 wt% glucose solution) using current methodology. Future efforts will be devoted on direct conversion of biomass (marine and terrestrial) to ethanol using the same strategy. Utilization of solar energy – which is renewable, clean, and sustainable – for bioethanol production is surely a significant leap towards the realization of an industrially-adoptable process.

Acknowledgements

The authors acknowledge the financial support from the Israel Science Foundation (ISF, Grant No. 598/12) and the Israel Ministry of Science, Technology and Space (Grant No. 3-9802 and 3-99763). The authors thank Mr Menachem Schneeberg, Head of Mechanical Workshop, Bar-Ilan University, for fabricating the solar reactor.

Notes and references

1 D. J. Hayes, S. Fitzpatrick, M. H. Hayes and J. R. Ross, *Biorefineries: Ind. Processes Prod.*, 2006, **1**, 139–164.
2 H. Su, G. Xu, H. Chen and Y. Xu, *ACS Sustainable Chem. Eng.*, 2015, **3**, 2002–2011.
3 A. Avami, *Renewable Sustainable Energy Rev.*, 2013, **26**, 761–768.
4 Y. H. P. Zhang, *Process Biochem.*, 2011, **46**, 2091–2110.
5 J. E. Anderson, D. M. DiCicco, J. M. Ginder, U. Kramer, T. G. Leone, H. E. Raney-Pablo and T. J. Wallington, *Fuel*, 2012, **97**, 585–594.
6 T. Hasunuma and A. Kondo, *Biotechnol. Adv.*, 2012, **30**, 1207–1218.
7 S. Nikolić, L. Mojović, M. Rakin, D. Pejin and J. Pejin, *Food Chem.*, 2010, **122**, 216–222.
8 P. Subhedar and P. R. Gogate, *Ind. Eng. Chem. Res.*, 2013, **52**, 11816–11828.
9 F. Talebnia, D. Karakashev and I. Angelidaki, *Bioresour. Technol.*, 2010, **101**, 4744–4753.
10 A. I. Galaction, A. M. Lupasteanu and D. Cascaval, *Open Syst. Biol. J.*, 2010, **3**, 9–20.
11 G. Francesca, F. Magherini, T. Gamberi, M. Borro, M. Simmaco and A. Modesti, *Biochim. Biophys. Acta, Proteins Proteomics*, 2010, **1804**, 1516–1525.
12 M. Akinori, I. Hiroyuki, K. Tsutomu and S. Shigeki, *Appl. Microbiol. Biotechnol.*, 2009, **84**, 37–53.
13 A. Pandey, *Biochem. Eng. J.*, 2003, **13**, 81–84.
14 B. Tabah, I. N. Pulidindi, V. R. Chitturi, L. M. R. Arava and A. Gedanken, *ChemSusChem*, 2015, **8**, 3497–3503.
15 B. Tabah, I. N. Pulidindi and A. Gedanken, *J. Bioprocess. Biotech.*, 2015, **5**, 232.
16 I. N. Pulidindi and A. Gedanken, *Springer Book Series-Production of Biofuels and Chemicals: Ultrasound*, ed. Z. Fang, L.-S. Fan, J. R. Grace, Y. Ni, N. R. Scott and R. L. Smith Jr, 2015, ch. 6, pp. 159–188.
17 I. N. Pulidindi, A. Gedanken, R. Schwarz and E. Sendersky, *Energy Fuels*, 2012, **26**, 2352–2356.
18 J. A. Choi, J. H. Hwang, B. A. Dempsey, R. A. Abou-Shanab, B. Min, H. Song and B. H. Jeon, *Energy Environ. Sci.*, 2011, **4**, 3513–3520.
19 K. Nakashima, K. Yamaguchi, N. Taniguchi, S. Arai, R. Yamada, S. Katahira and A. Kondo, *Green Chem.*, 2011, **13**, 2948–2953.
20 N. Saifuddin and R. Hussain, *J. Math. Stat.*, 2011, **7**, 198–206.
21 C. M. Neves, J. F. Granjo, M. G. Freire, A. Robertson, N. M. Oliveira and J. A. Coutinho, *Green Chem.*, 2011, **13**, 1517–1526.
22 J. Baeyens, Q. Kang, L. Appels, R. Dewil, Y. Lv and T. Tan, *Prog. Energy Combust. Sci.*, 2015, **47**, 60–88.
23 L. An and T. S. Zhao, *Energy Environ. Sci.*, 2011, **4**, 2213–2217.
24 L. An, T. S. Zhao and Y. S. Li, *Renewable Sustainable Energy Rev.*, 2015, **50**, 1462–1468.
25 L. An and T. S. Zhao, *Int. J. Hydrogen Energy*, 2011, **36**, 9994–9999.
26 T. Maiyalagan and K. Scott, *J. Power Sources*, 2010, **195**, 5246–5251.
27 E. Lee, I. S. Park and A. Manthiram, *J. Phys. Chem.*, 2010, **114**, 10634–10640.
28 K. Ye, D. Zhang, X. Wang, K. Cheng and D. Cao, *RSC Adv.*, 2015, **5**, 3239–3247.
29 L. Gu, N. Luo and G. H. Miley, *J. Power Sources*, 2007, **173**, 77–85.
30 A. Brouzgou, A. Podias and P. Tsiakaras, *J. Appl. Electrochem.*, 2013, **43**, 119–136.
31 C. V. Rao and B. Viswanathan, *J. Phys. Chem. C*, 2009, **113**, 18907–18913.
32 C. V. Rao and B. Viswanathan, *Electrochim. Acta*, 2010, **55**, 3002–3007.